Fizika Nizkikh Temperatur, 2005, v. 31, Nos. 8/9, p. 918–928

Localized-magnon states in strongly frustrated quantum spin lattices

J. Richter

Institut für Theoretische Physik, Universität Magdeburg
P.O. Box 4120, D-39016 Magdeburg, Germany
E-mail: Johannes.Richter@Physik.Uni-Magdeburg.DE

Received January 19, 2005

Recent developments concerning localized-magnon eigenstates in strongly frustrated spin lattices and their effect on the low-temperature physics of these systems in high magnetic fields are reviewed. After illustrating the construction and the properties of localized-magnon states we describe the plateau and the jump in the magnetization process caused by these states. Considering appropriate lattice deformations fitting to the localized magnons we discuss a spin-Peierls instability in high magnetic fields related to these states. Last but not least we consider the degeneracy of the localized-magnon eigenstates and the related thermodynamics in high magnetic fields. In particular, we discuss the low-temperature maximum in the isothermal entropy versus field curve and the resulting enhanced magnetocaloric effect, which allows efficient magnetic cooling from quite large temperatures down to very low ones.

PACS: 75.10.Jm, **75.45.+j**, 75.60.Ej, 75.50.Ee

1. Introduction

The interest in quantum spin antiferromagnetism has a very long tradition, see, e.g., Ref. 1. Stimulated by the recent progress in synthesizing magnetic materials with strong quantum fluctuations [2] particular attention has been paid on low-dimensional quantum magnets showing novel quantum phenomena like spin liquid phases, quantum phase transitions or plateaus and jumps in the magnetization process. However, quantum spin systems are of interest in their own right as examples of strongly interacting quantum many-body systems.

We know from the Mermin–Wagner theorem [3] that thermal fluctuations are strong enough to destroy magnetic long-range order (LRO) for Heisenberg spin systems in dimension $D < 3$ at any finite temperature T. For $T = 0$, where only quantum fluctuations are present, the situation seems to be more complicated. While for one-dimensional (1D) antiferromagnets, in general, the quantum fluctuations are strong enough to prevent magnetic LRO, the competition between interactions and fluctuations is well balanced in two dimensions and one meets magnetic LRO as well as magnetic disorder at $T = 0$ in dependence on details of the lattice [4–8]. It was pointed out many years ago by Anderson and Fazekas [9,10] that competition of magnetic bonds for instances due to triangular configurations of antiferromagnetically interacting spins may influence this balance and can lead to disordered ground-state phases in two-dimensional (2D) quantum antiferromagnets. In the context of spin glasses this competition of bonds, later on called frustration, was discussed in great detail. These studies on spin glasses have shown that frustration may have an enormous influence on ground state and thermodynamic properties [11] of spin systems.

The investigation of frustration effects in spin systems, especially in combination with strong quantum fluctuations, is currently a hot topic prime in solid state physics. We mention some interesting features like quantum disorder, incommensurate spiral phases, «*order by disorder*» phenomena to name a few, which might appear in frustrated systems. The theoretical study of frustrated quantum spin systems is challenging and is often faced with particular problems. While for unfrustrated systems a wide class of well developed many-body methods are available, at least some of them, e.g., the powerful Quantum Monte Carlo Method, fail for frustrated systems. Furthermore several important exact statements like the Marshall–Peierls sign rule [12] and the Lieb–Mattis

theorem [13] are not generally valid if frustration is present (see, e.g., [14,15]).

On the other hand, the investigation of strongly frustrated magnetic systems surprisingly led to the discovery of several new exact eigenstates. To find exact eigenstates of quantum many-body systems is, in general, a rare exception. For spin systems one has only a few examples. The simplest example for an exact eigenstate is the fully polarized ferromagnetic state, which becomes the ground state of an antiferromagnet in a strong magnetic field. Furthermore the one- and two-magnon excitations above the fully polarized ferromagnetic state also can be calculated exactly (see, e.g. [1]). An example for non-trivial eigenstates is Bethe's famous solution for the 1D Heisenberg antiferromagnet (HAFM) [16]. Some of the eigenstates found for frustrated quantum magnets are of quite simple nature and their physical properties, e.g., the spin correlation functions, can be calculated analytically. Note that such states are often eigenstates of the unfrustrated system, too, but they are irrelevant for the physics of the unfrustrated system if they are lying somewhere in the spectrum. However, the interest in these eigenstates comes from the fact that they may become ground states for particular values of frustration. Therefore these exact eigenstates play an important role either as ground states of real quantum magnets or at least as ground states of idealized models which can be used as reference states for more complex quantum spin systems.

Two well-known examples for simple eigenstates of strongly frustrated quantum spin systems are the Majumdar–Gosh state of the 1D $J_1 - J_2$ spin-half HAFM [17] and the orthogonal dimer state of the Shastry–Sutherland model [18]. Both eigenstates are product states built by dimer singlets. They become ground states only for strong frustration. These eigenstates indeed play a role in realistic materials. The Majumdar–Ghosh state has some relevance in quasi-1D spin-Peierls materials like $CuGeO_3$ (see, e.g., [19]). The orthogonal dimer state of the Shastry–Sutherland model is the magnetic ground-state of the quasi-two-dimensional $SrCu_2(BO_3)_2$ compound [20]. Other frustrated spin models in one, two or three dimensions are known which have also dimer-singlet product states as ground states (see, e.g., [21–24]). Note that these dimer-singlet product ground states have gapped magnetic excitations and lead therefore to a plateau in the magnetization m at $m = 0$. Recently it has been demonstrated for the 1D counterpart of the Shastry–Sutherland model [22, 25–27], that more general product eigenstates containing chain fragments of finite length can lead to an infinite series of magnetization plateaus [26]. Finally, we mention the so-called frustrated Heisenberg star where also exact statements on the ground state are known [28].

In this paper we review recent results concerning a new class of exact eigenstates appearing in strongly frustrated antiferromagnets, namely the so-called localized-magnon states. These states have been detected as ground states of certain frustrated antiferromagnets [29–31] in a magnetic field and their relevance for physical properties of a wide class of frustrated magnets has been discussed in [7, 29–37].

2. Localized magnon states

We consider a Heisenberg XXZ antiferromagnet for general spin quantum number s in a magnetic field h

$$\hat{H} = \sum_{\langle ij \rangle} J_{ij} \left\{ \Delta \hat{S}_i^z \hat{S}_j^z + \frac{1}{2} (\hat{S}_i^+ \hat{S}_j^- + \hat{S}_i^- \hat{S}_j^+) \right\} - h\hat{S}^z, \quad J_{ij} \geq 0. \tag{1}$$

The magnetization $M = \hat{S}^z = \sum_i \hat{S}_i^z$ commutes with the Hamiltonian and is used as a relevant quantum number to characterize the eigenstates of $\hat{H}$. Let us consider strong magnetic fields exceeding the saturation field $h_{\rm sat}$. Then the system is in the fully polarized ferromagnetic eigenstate $|\mathrm{FM}\rangle = |+s,+s,+s,+s \ldots\rangle$, which will be considered as the magnon vacuum state, i.e. $|0\rangle = |\mathrm{FM}\rangle$. The one-magnon states above this vacuum are given by

$$|1\rangle = \frac{1}{c} \sum_i^N a_i S_i^- |0\rangle; \; (\hat{H} - E_{FM})|1\rangle = w_i(\mathbf{k})|1\rangle, \tag{2}$$

where E_{FM} is the energy of the fully polarized ferromagnetic state $|\mathrm{FM}\rangle$ and c is a normalization constant. For several strongly frustrated lattices one observes flat dispersion modes $w_i(\mathbf{k}) = \mathrm{const}$ of the lowest branch. One example is shown in Fig. 1. Here we mention that there is some relation to the flat-band ferromagnetism in electronic systems discussed by Mielke and Tasaki, see [38–40].

Consequently, one can construct localized states by an appropriate superposition of extended states with different $\mathbf{k}$ vectors. The general form of these localized states can be written as [30,31]

$$|1\rangle_L = \frac{1}{c} \sum_i^N a_i \hat{S}_i^- |0\rangle = |\Psi_L\rangle |\Psi_R\rangle, \quad a_i \begin{cases} \neq 0 & \forall i \in L \;\; (\text{local}) \\ = 0 & \forall i \in R \;\; (\text{remainder}), \end{cases} \tag{3}$$

where $|\Psi_L\rangle$ belongs to the localized excitation living on the local region L and $|\Psi_R\rangle$ describes the fully po-

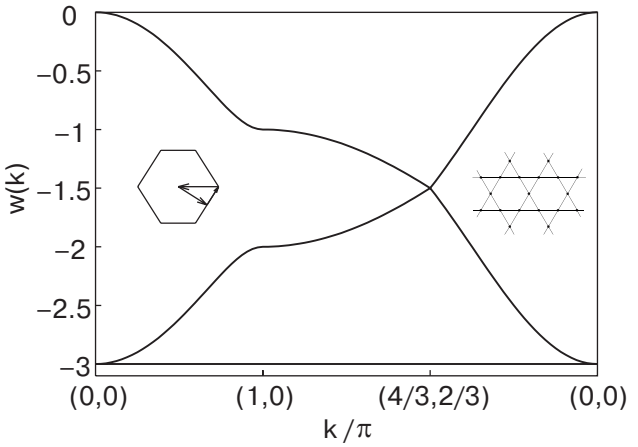

Fig. 1. Excitation energies $w_i(\mathbf{k})$ of the one-magnon states for the isotropic spin-half Heisenberg antiferromagnet (i.e., $J = 1$, $\Delta = 1$, $s = 1/2$ and $h = 0$ in Eq. (1)) on the kagomé lattice (right inset). The left inset shows the path in the Brillouin zone corresponding to k values used as x coordinate. This figure was provided by J. Schulenburg.

larized ferromagnetic remainder. We split the Hamiltonian into three parts $\hat{H} = \hat{H}_L + \hat{H}_{L-R} + \hat{H}_R$, where $\hat{H}_L$ contains all bonds J_{il} with $i, l \in L$, $\hat{H}_R$ contains all bonds J_{kj} with $k, j \in R$ and $\hat{H}_{L-R}$ contains all bonds J_{lk} with $l \in L$ and $k \in R$. The requirement that the localized-magnon state $|1\rangle_L$ is simultaneously an eigenstate of all three parts of the Hamiltonian, i.e. $\hat{H}_L|1\rangle_L = e_L|1\rangle_L$, $\hat{H}_R|1\rangle_L = e_R|1\rangle_L$ and $\hat{H}_{L-R}|1\rangle_L = e_{L-R}|1\rangle_L$, leads to two criteria for the exchange bonds J_{ij} [31], namely

$$\sum_{l \in L} J_{rl} a_l = 0 \quad \forall r \in R \tag{4}$$

and

$$\sum_{r \in R} J_{rl} = \text{const} \quad \forall l \in L. \tag{5}$$

Equation (4) represents a condition on the bond geometry, whereas Eq. (5) is a condition for the bond strengths and is automatically fulfilled in uniform lattices with equivalent sites. Note, however, that the second condition is not a necessary one, i.e., one can find models with eigenstates of form (3) violating (5), see [30]. This more general case appears if $|\Psi_L\rangle|\Psi_R\rangle$ is not an individual eigenstate of both $\hat{H}_L$ and $\hat{H}_{L-R}$ but of $(\hat{H}_{L-R} + \hat{H}_L)$. Hence, the geometry condition (4) is the criterion of major importance. A typical geometry fulfilling condition (4) is realized by an even polygon surrounded by isosceles triangles, see Fig. 2. The lowest one-magnon state living on an even polygon has coefficients a_i in $|1\rangle_L$ alternating in sign. But also finite strings of two or three sites attached by appropriate triangles can fulfill the criterion (4), see Fig. 2.

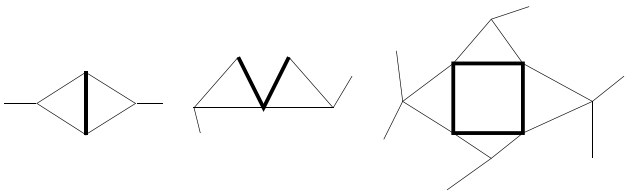

Fig. 2. Typical lattice geometries supporting the localized-magnon states (3). The magnon lives on the restricted area indicated by a thick line.

As an example we consider the HAFM (1) on the kagomé lattice [30], i.e., we have $J_{ij} = 1$ for nearest-neighbor (NN) bonds and $J_{ij} = 0$ else. Its one-magnon dispersion shown in Fig. 1 exhibits one flat mode. The resulting localized magnon lives on a hexagon, see Fig. 3,*a*. Its wave function is

$$|1\rangle_L^{\text{kagomé}} = \frac{1}{\sqrt{12S}} \sum_{\substack{i=1 \\ (i \in \text{hexagon})}}^{6} a_i \, \hat{S}_i^- |0\rangle, \quad a_i = (-1)^i. \tag{6}$$

Note that the number of hexagons $N/3$ corresponds to the number of states in the flat branch of $w(\mathbf{k})$. Because of the localized nature of the magnon we can put further such magnons on the lattice such that there is no interaction between them. The maximum filling $n_{\max}$ of the kagomé lattice with localized magnons is shown in Fig. 3,*b*. The resulting eigenstate is a magnon «crystal» state with $n_{\max} = N/9$ magnons and a magnetic unit cell three times as large as the geometric one. Therefore the states with $n = \{0, 1, 2, 3, \ldots, N/9\}$ localized magnons represent the class of exactly known product eigenstates with quantum numbers $M = S_z = Ns - n = \{Ns, Ns - 1, Ns - 2, \ldots, Ns - N/9\}$.

Due to the mutual independence of the localized magnons for $n \le n_{\max} \propto N$ the energy E_{loc} of the localized-magnon states is proportional to the number n of localized magnons, i.e. at $h = 0$ one has $E_{\text{loc}} = E_{FM} - n\varepsilon_1$, where E_{FM} is the energy of the

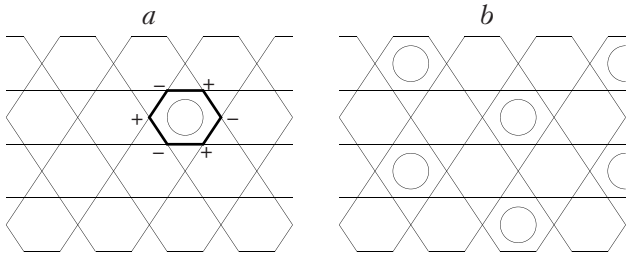

Fig. 3. Localized magnons on the kagomé lattice. One-magnon state indicated by a circle, the + and – signs correspond to the sign of the coefficients $a_i = \pm 1$, see Eq. (6) (*a*). Magnon crystal state corresponding to the maximum filling $n_{\max} = N/9$ of the kagomé lattice with localized magnons (circles) (*b*). The figures were taken from Ref. 30.

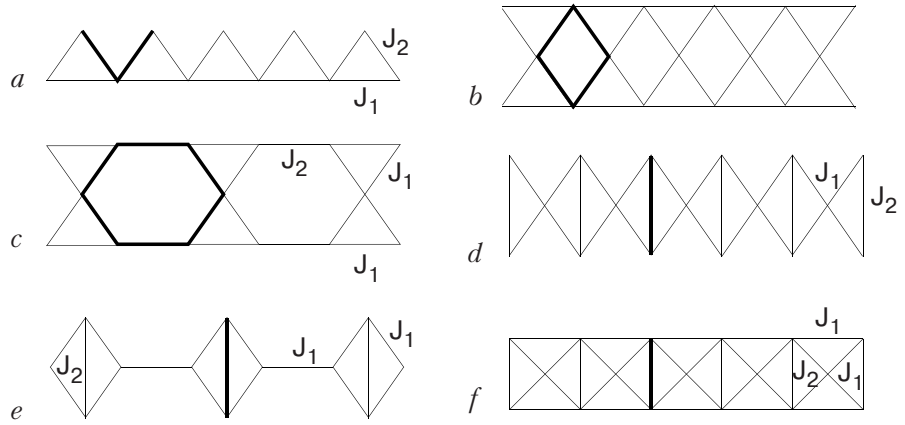

Fig. 4. One-dimensional systems with localized-magnon states. The magnons live on the restricted area indicated by a thick line: sawtooth chain [42,43] (*a*), kagomé chain I [44] (*b*), kagomé chain II [45] (*c*), diamond chain [46] (*d*), dimer-plaquette chain [22] (*e*), frustrated ladder [47] (*f*). Note that there are special restrictions for the exchange integrals to have localized-magnon states as lowest eigenstates in the corresponding sector of M.

fully polarized (vacuum) state and ε_1 is the energy gain by one magnon. As a results there is a simple linear relation between $E_{\rm loc}$ and the total magnetization M valid for all systems hosting localized magnons

$$E_{\rm loc}(M, h = 0) = -aN + bsM, \qquad (7)$$

where the parameters a and b depend on details of the system like the exchange constant J_{ij}, the anisotropy parameter Δ, the coordination number z of the lattice etc. For example for the isotropic spin-half HAFM with NN exchange J on the kagomé lattice one finds [30,35]

$$E_{\rm loc}(M, h = 0) = 2s^2NJ - 6snJ = -4s^2NJ + 6sJM. \qquad (8)$$

Note that also the spin–spin correlation functions of such states can be easily found [31].

For the physical relevance of these eigenstates it is crucial that they have lowest energy in the corresponding sector of M. Indeed this can be proved for quite general antiferromagnetic spin models [29,41].

Since the condition (4) for the existence of localized-magnon states is quite general, one can find a lot of magnetic systems in one, two and three dimensions having localized-magnon eigenstates [29–32,35–37,43].

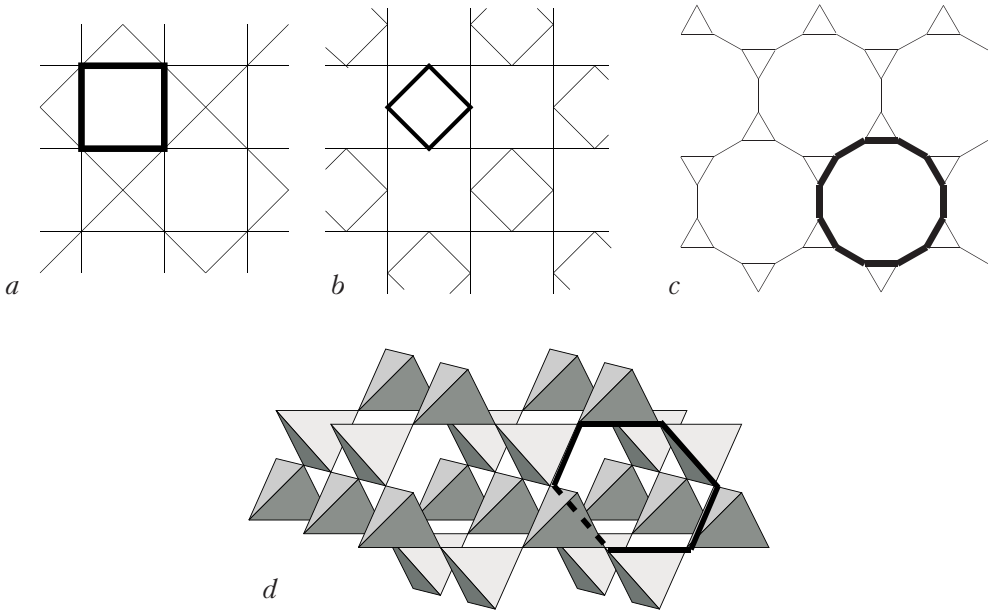

Fig. 5. Two- and three-dimensional antiferromagnets with localized-magnon states. The magnons live on the restricted area indicated by a thick line: planar pyrochlore (checkerboard) lattice [31,48] (*a*), square-kagomé lattice [37,49] (*b*), star lattice [7,36] (*c*), pyrochlore lattice [50] (*d*).

To illustrate that we show in Fig. 4 some 1D and in Fig. 5 some 2D and 3D antiferromagnetic spin lattices. But also for frustrated magnetic molecules localized-magnon states are observed [29].

3. Plateaus and jumps in the magnetization curve

As discussed in the previous Section the localized-magnon states are the lowest states in the corresponding sector of magnetization M. Hence they become ground states in appropriate magnetic fields h. Furthermore we stated that there is a linear relation between the energy of these states $E_{\rm loc}$ and M, cf. Eq. (7). Applying a magnetic field h the energy reads $E_{\rm loc}(M,h) = -aN + bsM - hM$ and one has a complete degeneracy of all localized-magnon states at the saturation field $h = h_{\rm sat} = bs$. As a result of this degeneracy the zero-temperature magnetization $m = M/(Ns)$ jumps between the saturation value $m = 1$ and the value $1 - n_{\rm max}/(Ns)$ corresponding to the maximum number $n_{\rm max}$ of independent localized magnons. Since $n_{\rm max}$ is proportional to N but independent of the spin quantum number s, the height of the jump $\delta m = n_{\rm max}/(Ns)$ goes to zero for s, i.e., the magnetization jump due to the localized-magnon states becomes irrelevant if the spins become classical.

We present in Fig. 6 two examples for the magnetization curves, further examples can be found in [7,27,31,36,37]. The jumps of height $\delta m = 1/2$ (sawtooth chain) and $\delta m = 2/7$ (kagomé lattice) are well pronounced. Furthermore we see a wide plateau at the foot of the jump for the sawtooth chain. Note that there are general arguments in favor of a plateau just below the jump [7,51,52]. Therefore we might expect a plateau preceeding the jump in all magnetic systems with localized magnon states. Though from Fig. 6 it remains unclear whether there is a plateau for the kagomé lattice, too, a more detailed analysis [32] yields indeed evidence for a finite plateau width of about $\delta h \sim 0.07J$.

4. Magnetic-field induced spin-Peierls instability in quantum spin lattices with localized-magnon states

The influence of a magnetoelastic coupling in frustrated antiferromagnets on their low-temperature properties is currently widely discussed. Lattice instabilities breaking the translational symmetry are reported for 1D, 2D as well 3D quantum spin systems, see e.g. [53]. In all those studies the lattice instability was considered at zero field. As discussed already in an early paper by Gross [54] a magnetic field usually acts against the spin-Peierls transition and might favor a uniform or incommensurate phase. In contrast to those findings, in this Section we discuss a lattice instability in frustrated spin lattices hosting localized magnons for which the magnetic field is essential [32].

First we point out that due to the localized nature of the magnons we have an inhomogeneous distribution of NN spin–spin correlations $\langle \hat{\mathbf{S}}_i \hat{\mathbf{S}}_j \rangle$ [31]. In case that one magnon is distributed uniformly over the lattice the deviation of the NN correlation from the

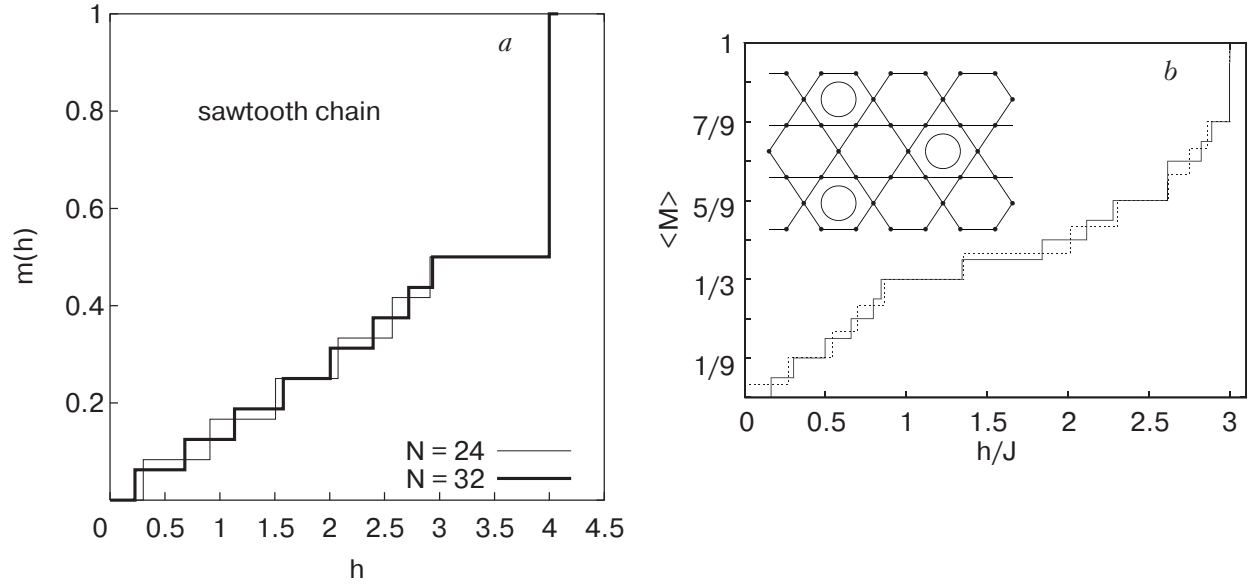

Fig. 6. Magnetization versus magnetic field h of the isotropic spin-half Heisenberg antiferromagnet. The sawtooth chain with $J_1 = 1$ and $J_2 = 2J_1$, cf. Fig. 4 (*a*). The figure was taken from Ref. 31. The kagomé lattice with $N = 27$ (dashed line) and 36 sites (solid line). The inset illustrates the «magnon crystal» state corresponding to maximum filling with localized magnons, where the location of the magnons is indicated by the circles in certain hexagons (*b*). The figure was taken from Ref. 8.

ferromagnetic value, i.e. the quantity $\langle \hat{\mathbf{S}}_i \hat{\mathbf{S}}_j \rangle - 1/4$, is of the order $1/N$. On the other hand for a localized magnon (3) we have along the polygon/line hosting the localized magnon actually in general a negative NN correlation $\langle \hat{\mathbf{S}}_i \hat{\mathbf{S}}_j \rangle$ and all other NN correlations are positive. For instance for the spin-half HAFM on the kagomé lattice the localized-magnon state (6) leads to $\langle \hat{\mathbf{S}}_i \hat{\mathbf{S}}_j \rangle = -1/12$ for neighboring sites i and j on a hexagon hosting a magnon and to $\langle \hat{\mathbf{S}}_i \hat{\mathbf{S}}_j \rangle = +1/6$ for neighboring sites i and j on an attaching triangle. Hence a deformation with optimal gain in magnetic energy will lead to an increase of antiferromagnetic bonds on the polygon/line hosting the localized magnon (i.e., hexagon for the kagomé lattice) and to a decrease of the bonds on the attaching triangles.

We shall discuss the situation for the isotropic spin-half HAFM on the kagomé lattice in more detail. A corresponding deformation which preserves the symmetry of the cell which hosts the localized magnon is shown in Fig. 7. To check the stability of the kagomé lattice with respect to a spin-Peierls mechanism we must compare the magnetic and the elastic energies. For the kagomé lattice the deformation shown in Fig. 7 leads to the following changes in the exchange interactions: $J \to (1 + \delta)J$ (along the edges of the hexagon) and $J \to (1 - \delta/2)J$ (along the two edges of the triangles attached to the hexagon), where the quantity δ is proportional to the displacement of the atoms and the change in the exchange integrals due to lattice distortions is taken into account in first order in δ. The magnetic energy (8) is lowered by distortions and becomes for one magnon and one corresponding distortion $E_{\rm loc}(n = 1, h = 0, \delta) = NJ/2 - 3J - 3\delta J/2$. Considering $n \le n_{\max}$ independent localized magnons and corresponding distortions the energy gain is then $e_{\rm mag} = -3n\delta J/2$. On the other hand the elastic energy in harmonic approximation increases according to $e_{\rm elast} \propto \delta^2$. Therefore a minimal total energy is obtained for a finite $\delta = \delta^* > 0$. For the kagomé lattice the elastic energy for one distorted cell is $e_{\rm elast} = 9\gamma\delta^2$ (the parameter γ is proportional to the elastic constant of the lattice). If the localized-magnon states are the ground states of the systems then we have a favorable spin-Peierls distortion with $\delta^* = J/(12\gamma)$. As discussed in the previous Section we expect a plateau at the foot of the magnetization jump. The spin-Peierls distortion due to localized-magnon states then takes place for the values of the magnetic field belonging to this plateau.

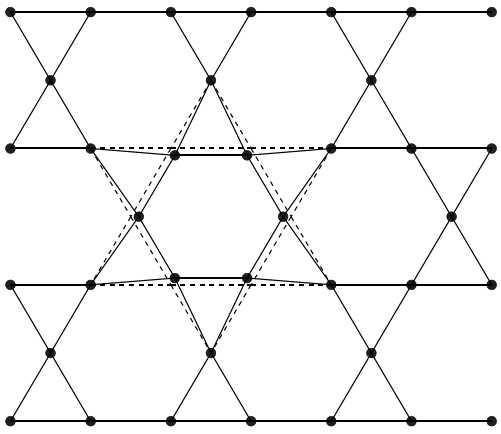

Fig. 7. Kagomé lattice with one distorted hexagon which can host localized magnons. The parts of the lattices before distortions are shown by dashed lines. All bonds in the lattices before distortions have the same length. The figure was taken from Ref. 32.

Now the question arises whether the lattice distortion under consideration is stable below and above this plateau, i.e., for $M < N/2 - n_{\max}$ and $M = N/2$. It is easy to check that the lattice distortion illustrated in Fig. 7 is not favorable for the fully polarized vacuum state, i.e. for $M = N/2$. For magnetizations M below this plateau, we are not able to give a rigorous answer but numerical results for finite kagomé lattices of size $N = 18, 27, 36, 45, 54$ indicate that there is no spin-Peierls deformation adopting the lattice distortion shown in Fig. 7 for $M < N/2 - n_{\max}$ (for more details, see [32]).

We mention that the scenario discussed above basically remains unchanged for the anisotropic Hamiltonian (1) with $\Delta \neq 1$ and also for spin quantum number $s > 1/2$ [32].

From the experimental point of view the discussed effect should most spectacularly manifest itself as a hysteresis in the magnetization and the deformation of kagomé-lattice antiferromagnets in the vicinity of the saturation field. We emphasize that the discussed spin-Peierls instability in high magnetic fields may appear in the whole class of frustrated quantum magnets in one, two and three dimensions hosting independent localized magnons provided it is possible to construct a lattice distortion preserving the symmetry of the localized-magnon cell.

5. Finite low-temperature entropy and enhanced magnetocaloric effect in the vicinity of the saturation field

It is well-known that strongly frustrated Ising or classical Heisenberg spin systems may exhibit a huge ground state degeneracy, see e.g. [5–7,55–58]. For *quantum* systems due to fluctuations the degeneracy found for classical systems is often lifted and the quantum ground state is unique (so-called «*order from disorder*» phenomenon [60,61]). However, highly frustrated antiferromagnetic quantum spin lat-

tices hosting localized magnons are an example where one finds a huge ground state degeneracy in a *quantum* system. As discussed in Sec. 3 the localized-magnon states become degenerate at saturation field. As pointed out first in [7] the degeneracy grows exponentially with system size N. In more detail this huge degeneracy and its consequence for the low temperature physics were discussed in [33–35].

For some of the spin systems hosting localized magnons the ground state degeneracy at saturation and therefore the residual entropy at zero temperature can be calculated exactly by mapping the localized-magnon problem onto a related lattice gas model of hard-core objects [33–35]. These lattice gas models of hard-core objects have been studied over the last decades in great detail (see, e.g., [59]). Let us illustrate this for the sawtooth chain. Here the local areas where the magnons can live are the valleys of the sawtooth chain, see Fig. 4,*a*. Because a certain local area of the lattice can be occupied by a magnon or not, the degeneracy of the groundstate at saturation, $\mathcal{W}$, grows exponentially with N giving rise to a finite zero-temperature entropy per site at saturation

$$\frac{S}{N} = \lim_{N\to\infty} \frac{1}{N} \log \mathcal{W} > 0. \qquad (9)$$

Now we map the original lattice which hosts localized magnons onto an auxiliary lattice which is occupied by hard-core objects, which are rigid monomers and dimers in the case of the sawtooth chain, see Fig. 8. The auxiliary chain (Fig. 8,*b*) consists of $\mathcal{N} = N/2$ sites which may be filled either by rigid monomers or by rigid dimers occupying two neighboring sites. The limiting behavior of $\mathcal{W}$ for $\mathcal{N} \to \infty$ was found by Fisher many years ago [59]

$$\mathcal{W} = \exp\left(\log \frac{1+\sqrt{5}}{2} \mathcal{N} \right) \approx \exp(0.240606N) \to$$

$$\to \frac{S}{N} = 0.240606. \qquad (10)$$

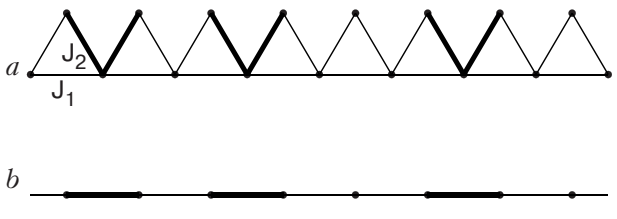

Fig. 8. The sawtooth chain which hosts three localized magnons at fat V parts (*a*) and the auxiliary lattice used for the exact calculation of the groundstate degeneracy at saturation (*b*). The localized magnons are eigenstates for $J_2 = \sqrt{2(1+\Delta)}J_1$ [30]. The figure was taken from Ref. 35.

The relevance of this result for experimental studies emerges at low but finite temperatures. In Ref. 33 this mapping was used to obtain a quantitative description of the low-temperature magnetothermodynamics in the vicinity of the saturation field of the quantum antiferromagnet on the kagomé lattice and on the sawtooth chain.

In what follows we report on the extension of the analytical findings for the zero-temperature entropy at the saturation field to finite temperatures and to arbitrary magnetic fields using exact diagonalization data for the sawtooth chain of up to $N = 20$ sites [34,35]. In Fig. 9,*a* we show the isothermal entropy versus magnetic field for several temperatures. The presented results show that for several magnetic fields below saturation $h < h_{\rm sat}$ one has a two-fold or even a three-fold degeneracy of the energy levels leading in a finite system to a finite zero-temperature entropy per site. Correspondingly one finds in Fig. 9,*a* (upper panel) a peaked structure and moreover a plateau-like area just below $h_{\rm sat}$. However, it is clearly seen in Fig. 9,*a* (upper panel) that the height of the peaks and of the plateau decreases with system size N leading to $\lim_{N\to\infty} S/N = 0$ at $T = 0$ for $h < h_{\rm sat}$ and $h > h_{\rm sat}$. Only the peak at $h = h_{\rm sat} = 4$ is independent of N and remains finite for $N \to \infty$. At finite but low temperatures this peak survives as a well-pronounced maximum and it only disappears if the temperature is of the order of the exchange constant, see Fig. 9,*a* (lower panel). Note that the value of the entropy at saturation, which agrees with the analytical prediction (10), is almost temperature independent up to about $T \approx 0.2$. Thus, the effect of the independent localized magnons leading to a finite residual zero-temperature entropy is present at finite temperatures $T \lesssim 0.2$ producing a noticeable maximum in the isothermal entropy curve at the saturation field. We mention that the numerical results for higher spin quantum numbers s suggest that the enhancement of the entropy at saturation for finite temperatures becomes less pronounced with increasing s.

With respect to the experimental observation of the maximum in the low-temperature entropy at the saturation field in real compounds we are faced with the situation that the condition on bond strengths, see Eq. (4), under which the localized-magnon states become the exact eigenstates are certainly not strictly fulfilled. For the considered isotropic spin-half HAFM on the sawtooth chain this condition is fulfilled for $J_2 = 2J_1$, see Fig. 9,*a*. Based on the numerical calculations one is able to discuss the «stability» of the maximum in the entropy against deviation from the perfect condition for bond strengths. In Fig. 9,*b* we show the field dependence of the entropy at low temperatures for the sawtooth

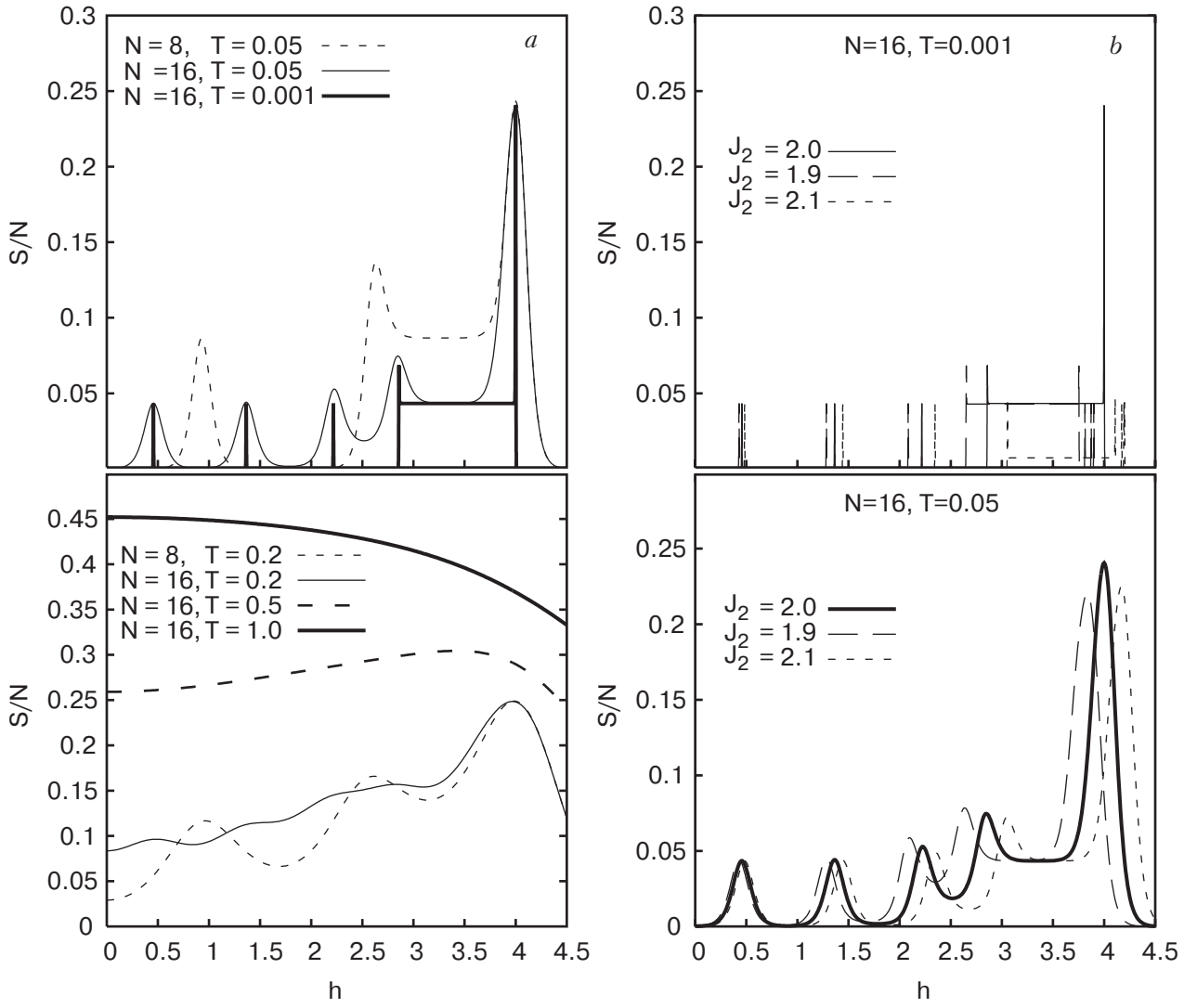

Fig. 9. Field dependence of the isothermal entropy per site for the Heisenberg antiferromagnet on the sawtooth chain of different length ($s = 1/2$, $\Delta = 1$). $J_1 = 1$, $J_2 = 2$, i.e., the condition for bond strengths (4) is fulfilled and the localized-magnon states are exact eigenstates (*a*). Influence of a deviation from the perfect condition for bond strengths (*b*). The figures were taken from Ref. 35.

chain of $N = 16$ sites with $J_1 = 1$ and $J_2 = 1.9$ and $J_2 = 2.1$. Since the degeneracy of the ground state at saturation is lifted when $J_2 \neq 2J_1$, the entropy at saturation at very low temperatures (long-dashed and short-dashed curves in the upper panel of Fig. 9,*b*) is not enhanced at the saturation field. However, the initially degenerate energy levels remain close to each other, if J_2 only slightly deviates from the perfect value $2J_1$. Therefore with increasing temperature those levels become accessible for the spin system and one obtains again a maximum in the entropy in the vicinity of saturation at low but nonzero temperatures, see lower panel in Fig. 9,*b* (long-dashed and short-dashed peaks in the vicinity of saturation). We emphasize that the low-temperature maximum of S/N at saturation is a generic effect for strongly frustrated quantum spin lattices which may host independent localized magnons.

Let us remark that the ground-state degeneracy problem of antiferromagnetic Ising lattices in the critical magnetic field (i.e., at the spin-flop transition point), which obviously do not contain quantum fluctuations, has been discussed in the literature, see, e.g., [62].

It has been pointed out very recently by Zhitomirsky and Honecker [34,63] that the most spectacular effect accompanying a maximum in the isothermal entropy $S(h)$ is an enhanced magnetocaloric effect. Indeed the cooling rate for an adiabatic (de)magnetization process is proportional to the derivative of the isothermal entropy with respect to the magnetic field

$$\left(\frac{\partial T}{\partial h}\right)_S = -T\frac{(\partial S/\partial h)_T}{C}, \qquad (11)$$

where C is the specific heat. Again one can calculate the field dependence of the temperature for an adiabatic (de)magnetization process for finite systems by exact diagonalization. Some results for the isotropic spin-half HAFM on the sawtooth chain are shown in Fig. 10. The lowest curves in Fig. 10 belongs to $S/N = 0.05$ and $N = 12, 16, 20$, respectively. The other curves correspond to $S/N = 0.1, 0.15, \ldots, 0.4, 0.45$. The magnetocaloric effect is largest in the vicinity of the saturation field. In particular, a demagnetization coming from magnetic fields larger than $h_{\rm sat}$ is very efficient. If one starts for $h > h_{\rm sat}$ with an entropy lower than the residual entropy at $h_{\rm sat}$, $S/N = 0.240606$ (see Eq. (10)), then one observes even a cooling to $T \to 0$ as $h \to h_{\rm sat}$. Thus frustrated magnetic systems hosting localized magnons allow magnetic cooling from quite large T down to very low temperatures. We mention, that the results shown in Fig. 10 also clearly demonstrate that finite-size effects are very small for $h \gtrsim h_{\rm sat}$ at any temperature. Therefore the above discussion is valid also for large systems $N \to \infty$.

6. Summary

We have reviewed recent results [29–37] on exact eigenstates constructed from localized magnons which appear in a class of frustrated spin lattices. For these eigenstates several quantities like the energy and the spin-spin correlation can be calculated analytically. The physical relevance of the localized-magnon eigenstates emerges at high magnetic fields where they can become ground states of the spin system.

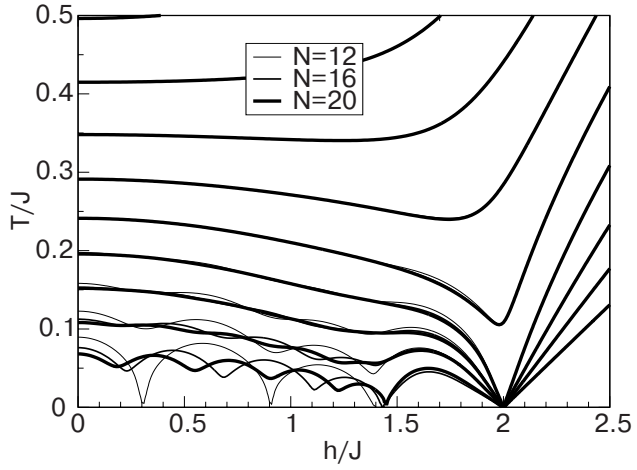

Fig. 10. Lines of constant entropy versus field (i.e., adiabatic (de)magnetization curves) for the Heisenberg antiferromagnet on the sawtooth chain of different length ($s = 1/2$, $\Delta = 1$, $J_1 = J/2$, $J_2 = J$). The figure was taken from Ref. 34 with friendly permission of A. Honecker.

For frustrated magnetic systems having localized-magnon ground states several interesting physical effects associated with this states may occur. First one finds a macroscopic jump in the zero-temperature magnetization curve at the saturation field $h_{\rm sat}$. This jump is a true quantum effect which vanishes if the spins become classical ($s \to \infty$). At the foot of the jump one can expect a plateau in the magnetization curve.

Since all localized-magnon states have the same energy at $h = h_{\rm sat}$ a huge degeneracy of the groundstate at saturation is observed which increases exponentially with system size N thus leading to a nonzero residual zero-temperature entropy. For some of the frustrated spin models hosting localized magnons the residual entropy at saturation field can be estimated exactly. At finite temperatures T the localized-magnon states produce a maximum in the isothermal entropy versus field curve in the vicinity of the saturation field for not too large T. This maximum in the isothermal entropy at $h_{\rm sat}$ leads to an enhanced magnetocaloric effect. If one starts for $h > h_{\rm sat}$ with an entropy lower than the residual entropy at $h_{\rm sat}$ then one observes even a cooling to $T \to 0$ as $h \to h_{\rm sat}$. This may allow cooling from quite large T down to very low temperatures.

Last but not least the localized-magnon states may lead to a spin-Peierls instability in strong magnetic fields, for instance for the antiferromagnetic kagomé spin lattice. For this system the magnetic-field driven spin-Peierls instability breaks spontaneously the translational symmetry of the kagomé lattice and appears only in a certain region of the magnetic field near saturation.

We emphasize that the reported effects are generic in highly frustrated magnets. To observe them in experiments one needs frustrated magnets with small spin quantum number s and sufficiently small exchange coupling strength J to reach the saturation field. There is an increasing number of synthesized quantum frustrated spin lattices, e.g., quantum antiferromagnets with a kagomé-like structure [64–67]. Though such materials often do not fit perfectly to the lattice geometry having localized-magnon ground states, the physical effects based on localized magnons states may survive in non-ideal geometries (see Sec. 5), which may open the window to the experimental observation of the theoretically predicted effects.

The author is indebted to O. Derzhko, A. Honecker, H.-J. Schmidt, J. Schnack, and J. Schulenburg for the fruitful collaboration in the field of local-

ized-magnon states in frustrated antiferromagnets. Most of the results discussed in the paper are based on common publications with these colleagues. In particular, I thank J. Schulenburg for many valuable discussions and hints. Furthermore I thank H. Frahm for directing my attention to the flat-band ferromagnetism. I also acknowledge the support from the Deutsche Forschungsgemeinschaft (project No. Ri615/12-1).

1. D.C. Mattis, *The Theory of Magnetism I*, Springer-Verlag Berlin (1991).
2. P. Lemmens and P. Millet, in: *Quantum Magnetism*, *Lecture Notes in Physics* **645**, U. Schollwöck, J. Richter, D.J.J. Farnell, and R.F. Bishop (eds.), Springer-Verlag, Berlin (2004), p. 433.
3. N.D. Mermin and H. Wagner, *Phys. Rev. Lett.* **17**, 1133 (1966).
4. C. Lhuillier, P. Sindzingre, and J.-B. Fouet, *Can. J. Phys.* **79**, 1525 (2001).
5. R. Moessner, *Can. J. Phys.* **79**, 1283 (2001).
6. G. Misguich and C. Lhuillier, in: *Frustrated Spin Systems*, H.T. Diep (ed.), World-Scientific (2005).
7. J. Richter, J. Schulenburg, and A. Honecker, in: *Quantum Magnetism in Two Dimensions: From Semi-Classical N'eel Order to Magnetic Disorder*; in: *Quantum Magnetism*, *Lecture Notes in Physics* **645**, U. Schollwöck, J. Richter, D.J.J. Farnell, and R.F. Bishop (eds.), Springer-Verlag, Berlin (2004), p. 85; see also *cond-mat/0412662*.
8. A. Honecker, J. Schulenburg, and J. Richter, *J. Phys.: Condens. Matter* **16**, S749 (2004).
9. P.W. Anderson, *Mater. Res. Bull.* **8**, 153 (1973).
10. P. Fazekas and P.W. Anderson, *Philos. Mag.* **30**, 423 (1974).
11. K. Binder and A.P. Young, *Rev. Mod. Phys*. **58**, 801 (1986).
12. W. Marshall, *Proc. Roy. Soc*. **A232**, 48 (1955).
13. E. Lieb and D. Mattis, *Ordering Energy Levels of Interacting Spin Systems*, *J. Math. Phys.* **3**, 749 (1962).
14. J. Richter, N.B. Ivanov, and K. Retzlaff, *Europhys. Lett*. **25**, 545 (1994).
15. J. Richter, N.B. Ivanov, K. Retzlaff, and A. Voigt, *J. Magn. Magn. Matter* **140-144**, 1611 (1995).
16. H.A. Bethe, *Z. Phys.* **71**, 205 (1931).
17. C.K. Majumdar and D.K. Ghosh, *J. Math. Phys.* **10**, 1399 (1969).
18. B.S. Shastry and B. Sutherland, *Physica* **B108**, 1069 (1981).
19. D. Poilblanc, J. Riera, C.A. Hayward, C. Berthier, and M. Horvatic, *Phys. Rev.* **B55**, R11941 (1997).
20. S. Miyahara and K. Ueda, *Phys. Rev. Lett.* **82**, 3701 (1999).
21. A. Pimpinelli, *J. Phys.: Condens. Matter* **3**, 445 (1991).
22. N.B. Ivanov and J. Richter, *Phys. Rev.* **A232**, 308 (1997); J. Richter, N.B. Ivanov and J. Schulenburg, *J. Phys.: Condens. Matter* **10**, 3635 (1998).
23. K. Ueda and S. Miyahara, *J. Phys.: Condens. Matter* **11**, L175 (1999).
24. H.-J. Schmidt, *J. Phys.* **A38**, 2133 (2005).
25. A. Koga, K. Okunishi, and N. Kawakami, *Phys. Rev.* **B62**, 5558 (2002); A. Koga and N. Kawakami, *Phys. Rev.* **B65**, 214415 (2002).
26. J. Schulenburg and J. Richter, *Phys. Rev.* **B65**, 054420 (2002).
27. J. Schulenburg and J. Richter, *Phys. Rev.* **B66**, 134419 (2002).
28. J. Richter and A. Voigt, *J. Phys*. **A27**, 1139 (1994); J. Richter, A. Voigt, and S. Krüger, *J. Magn. Magn. Matter* **140-144**, 1497 (1995); J. Richter, A. Voigt, and S. Krüger, *J. Phys*. **A29**, 825 (1996).
29. J. Schnack, H.-J. Schmidt, J. Richter, and J. Schulenburg, *Eur. Phys. J.* **B24**, 475 (2001).
30. J. Schulenburg, A. Honecker, J. Schnack, J. Richter, and H.-J. Schmidt, *Phys. Rev. Lett.* **88**, 167207 (2002).
31. J. Richter, J. Schulenburg, A. Honecker, J. Schnack, and H.-J. Schmidt, *J. Phys.: Condens. Matter* **16**, S779 (2004).
32. J. Richter, O. Derzhko, and J. Schulenburg, *Phys. Rev. Lett.* **93**, 107206 (2004).
33. M.E. Zhitomirsky and H. Tsunetsugu, *Phys. Rev.* **B70**, 100403(R) (2004).
34. M.E. Zhitomirsky and A. Honecker, *J. Stat. Mech.: Theor. Exp.*, P07012 (2004).
35. O. Derzhko and J. Richter, *Phys. Rev.* **B70**, 104415 (2004).
36. J. Richter, J. Schulenburg, A. Honecker, and D. Schmalfuß, *Phys. Rev.* **B70**, 174454 (2004).
37. J. Richter, J. Schulenburg, P. Tomczak, and D. Schmalfuß, *cond-mat/0411673* (2004), submitted to: *Phys. Rev. B*.
38. A. Mielke, *J. Phys*. **A24**, 3311 (1991).
39. H. Tasaki, *Phys. Rev. Lett*. **69**, 1608 (1992).
40. A. Mielke and H. Tasaki, *Commun. Math. Phys.* **158**, 341 (1993).
41. H.-J. Schmidt, *J. Phys*. **A35**, 6545 (2002).
42. T. Nakamura and K. Kubo, *Phys. Rev.* **B53,** 6393 (1996); D. Sen, B. S. Shastry, R. E. Walstedt, and R. Cava, *Phys. Rev.* **B53,** 6401 (1996).
43. V. Ravi Chandra, D. Sen, N.B. Ivanov, and J. Richter, *Phys. Rev.* **B69**, 214406 (2004).
44. Ch. Waldtmann, H. Kreutzmann, U. Schollwöck, K. Maisinger, and H.-U. Everts, *Phys. Rev.* **B62,** 9472 (2000).
45. P. Azaria, C. Hooley, P. Lecheminant, and A.M. Tsvelik, *Phys. Rev. Lett.* **81,** 1694 (1998).
46. H. Niggemann, G. Uimin, and J. Zittartz, *J. Phys.: Condens. Matter* **9**, 9031 (1997).
47. F. Mila, *Eur. Phys. J.* **B6,** 201 (1998), A. Honecker, F. Mila, and M. Troyer, *Eur. Phys. J.* **B15,** 227 (2000).
48. S. E. Palmer and J. T. Chalker, *Phys. Rev.* **B64,** 094412 (2001).

49. R. Siddharthan and A. Georges, *Phys. Rev.* **B65**, 014417 (2002); P. Tomczak and J. Richter, *J. Phys.* **A36**, 5399 (2003).
50. B. Canals and C. Lacroix, *Phys. Rev. Lett.* **80**, 2933 (1998).
51. T. Momoi and K. Totsuka, *Phys. Rev.* **B61**, 3231 (2000).
52. M. Oshikawa, *Phys. Rev. Lett.* **84**, 1535 (2000).
53. S.-H. Lee, C. Broholm, T.H. Kim, W. Ratcliff II, and S-W. Cheong, *Phys. Rev. Lett.* **84,** 3718 (2000); Y. Yamashita and K. Ueda, *Phys. Rev. Lett.* **85,** 4960 (2000); A. Keren and J.S. Gardner, *Phys. Rev. Lett.* **87,** 177201 (2001); F. Becca and F. Mila, *Phys. Rev. Lett.* **89,** 037204 (2002); P. Carretta, N. Papinutto, C.B. Azzoni, M.C. Mozzati, E. Pavarini, S. Gonthier, and P. Millet, *Phys. Rev.* **B66,** 094420 (2002); O. Tchernyshyov, R. Moessner, and S.L. Sondhi, *Phys. Rev. Lett.* **88,** 067203 (2002); F. Becca, F. Mila, and D. Poilblanc, *Phys. Rev. Lett.* **91,** 067202 (2003).
54. M.C. Gross, *Phys. Rev.* **B20,** 4606 (1979).
55. G.H. Wannier, *Phys. Rev.* **79**, 357 (1950).
56. R. Moessner and S.L. Sondhi, *Phys. Rev.* **B63,** 224401 (2001).
57. M.E. Zhitomirsky, *Phys. Rev. Lett.* **88,** 057204 (2002).
58. M. Udagawa, M. Ogata, and Z. Hiroi, *J. Phys. Soc. Jpn*. **71,** 2365 (2002).
59. M.E. Fisher, *Phys. Rev.* **124**, 1664 (1961); R.J. Baxter, I.G. Enting, and S.K. Tsang, *J. Stat. Phys*. **22**, 465 (1980); R.J. Baxter and S.K. Tsang, *J. Phys*. **A13**, 1023 (1980); *R.J*. Baxter, *J. Phys*. **A13**, L61 (1980); R.J. Baxter, *Exactly Solved Models in Statistical Mechanics*, Academic Press, London (1982); R.J. Baxter, *Ann. Combinatorics* **3**, 191 (1999).
60. J. Villain, R. Bidaux, J.P. Carton, and R. Conte, *J. Phys*. **41**, 1263 (1980).
61. E.F. Shender, *Zh. Eksp. Teor. Fiz*. **83**, 326 (1982) (*Sov. Phys. JETP* **56**, 178 (1982)).
62. B.D. Metcalf and C.P. Yang, *Phys. Rev.* **B18,** 2304 (1978).
63. M.E. Zhitomirsky, *Phys. Rev.* **B67,** 104421 (2003).
64. A.P. Ramirez, B. Hessen, and M. Winklemann, *Phys. Rev. Lett.* **84**, 2957 (2000).
65. Zenji Hiroi, Masafumi Hanawa, Naoya Kobayashi, Minoru Nohara, Hidenori Takagi, Yoshitomo Kato, and Masashi Takigawa, *J. Phys. Soc. Jpn*. **70,** 3377 (2001).
66. A. Fukaya, Y. Fudamoto, I.M. Gat, T. Ito, M.I. Larkin, A.T. Savici, Y.J. Uemura, P.P. Kyriakou, G.M. Luke, M.T. Rovers, K.M. Kojima, A. Keren, M. Hanawa, and Z. Hiroi, *Phys. Rev. Lett.* **91,** 207603 (2003).
67. D. Bono, P. Mendels, G. Collin, and N. Blanchard, *Phys. Rev. Lett.* **92**, 217202 (2004).